Elsevier Editorial System(tm) for Annals of Anatomy

Manuscript Draft

Manuscript Number:

Title: Normal microscopic anatomy of equine body and limb skin: morphometrical and immunohistochemical study.

Article Type: VSI: Animal Anatomy III - Original paper

Keywords: Horse skin, differentiation markers, epithelial thickness, proliferation index, mast cells

Corresponding Author: Dr. Vincenzo Miragliotta, DVM, PhD

Corresponding Author's Institution: University of Pisa

First Author: Elin Jørgensen

Order of Authors: Elin Jørgensen; Giulia Lazzarini; Andrea Pirone; Stine Jacobsen; Vincenzo Miragliotta, DVM, PhD

Abstract: Introduction: Information on microscopic anatomy of equine skin is sparse. In horses, limb wounds often become chronic and/or non-healing whereas body wounds heal normally. These dissimilarities in healing patterns might be a product of different phenotypic characteristics of body and limb skin. The objective of this study was to investigate microscopic anatomy, epithelial thickness, keratinocyte proliferation and differentiation as well as presence of mast cells in normal equine body and limb skin.
Materials and methods: The study involved body and limb skin biopsies from six horses. Histological characteristics of the epidermis were assessed and epithelial thickness measured. Immunuhistochemistry was performed to investigate epidermal differentiation patterns of cytokeratin (CK) 10, CK14, CK16, loricrin, and peroxisome proliferator-activated receptor alpha (PPAR-α), epidermal proliferation (Ki-67 iimunostaining), and morphometric analysis of mast cells distribution in the skin.
Results: Epidermis was significantly thicker in the limb skin compared to body skin ($P < 0.01$). Epidermal proliferation and CK distribution did not show differences in the two anatomical areas. Loricrin presence was focally found in the spinous layer in four out of six limb skin samples but not in body skin samples. Tryptase positive mast cells were detected in the dermis and their density (cell/mm2) was not different between body and limb.
Discussion and conclusion: Here we report for the first time the normal distribution of CK10, CK14, CK16, PPAR-α, and loricrin in equine limb and body skin as well as epidermal proliferation rate and mast cell count. It will be relevant to investigate distribution of the investigated epithelial differentiation markers and the role of mast cells during equine wound healing and/or other skin diseases.

Cover Letter

To the editor

Annals of Anatomy

Dear editor, please find enclosed the manuscript entitled “Normal microscopic anatomy of equine body and limb skin: a morphometrical and immunohistochemical study” I am pleased to submit for your consideration for publication in the upcoming special issue on Animal Anatomy.

Although horses suffer major problems in healing skin wounds located in the metacarpal/metatarsal area, the microscopic anatomy of equine skin is poorly described with the most prominent work published more than 40 years ago. Here we report for the first time the normal distribution of CK10, CK14, CK16, PPAR-α, and loricrin in equine limb and body skin as well as epidermal proliferation rate and mast cell count. This study may serve as a basis for other studies conducted on equine skin using these markers.

All authors have approved the final version of the article. On behalf of all the authors I declare that the work has not been published and is not being considered for publication elsewhere.

Best regards

Vincenzo Miragliotta

Normal microscopic anatomy of equine body and limb skin: a morphometrical and immunohistochemical study.

Elin Jørgensen[a], Giulia Lazzarini[b], Andrea Pirone[b], Stine Jacobsen[a], Vincenzo Miragliotta[b].

[a]Department of Veterinary Clinical Sciences, University of Copenhagen, Højbakkegaard Alle 5, DK-2630 Taastrup, Denmark

[b]Department of Veterinary Sciences, University of Pisa, viale delle Piagge 2, 56124 Pisa, Italy

Corresponding author: Vincenzo Miragliotta, DVM, PhD. Department of Veterinary Sciences, University of Pisa, Viale delle Piagge 2, 56124 Pisa, Italy, tel. +39-050-2216865, fax. +39-050-2210655, vincenzo.miragliotta@unipi.it

Abstract

Introduction: Information on microscopic anatomy of equine skin is sparse. In horses, limb wounds often become chronic and/or non-healing whereas body wounds heal normally. These dissimilarities in healing patterns might be a product of different phenotypic characteristics of body and limb skin. The objective of this study was to investigate microscopic anatomy, epithelial thickness, keratinocyte proliferation and differentiation as well as presence of mast cells in normal equine body and limb skin.

Materials and methods: The study involved body and limb skin biopsies from six horses. Histological characteristics of the epidermis were assessed and epithelial thickness measured. Immunuhistochemistry was performed to investigate epidermal differentiation patterns of cytokeratin (CK) 10, CK14, CK16, loricrin, and peroxisome proliferator-activated receptor alpha (PPAR-α), epidermal proliferation (Ki-67 iimunostaining), and morphometric analysis of mast cells distribution in the skin.

Results: Epidermis was significantly thicker in the limb skin compared to body skin ($P < 0.01$). Epidermal proliferation and CK distribution did not show differences in the two anatomical areas. Loricrin presence was focally found in the spinous layer in four out of six limb skin samples but not in body skin samples. Tryptase positive mast cells were detected in the dermis and their density (cell/mm^2) was not different between body and limb.

Discussion and conclusion: Here we report for the first time the normal distribution of CK10, CK14, CK16, PPAR-α, and loricrin in equine limb and body skin as well as epidermal proliferation rate and mast cell count. It will be relevant to investigate distribution of the investigated epithelial differentiation markers and the role of mast cells during equine wound healing and/or other skin diseases.

Keywords: skin, differentiation markers, epithelial thickness, proliferation index, horse, mast cells

1. Introduction

Skin is a complex organ that contains several cell populations (Jatana and DeLouise, 2014). The microscopic anatomy of equine skin is poorly described with the most prominent work published more than 40 years ago (Talukdar et al., 1972a, b).

Horses are prone to different skin diseases like traumatic wounds, sarcoids, tumors, allergies and atopy (Wobeser, 2015). Difficult-to-heal wounds are common among horses (Owen et al., 2012; Theoret et al., 2016) and were in 2015 estimated to account for 16% of euthanasia in adult horses in the US (Anonymous, 2015). Specifically, healing of wounds located in the metacarpal/metatarsal area in horses is often fraught with complications compared to wounds located at the body (Jorgensen et al., 2017; Sørensen et al., 2014; Theoret et al., 2001). Impaired wound healing in equine limb wounds is characterized with greater retraction, premature cessation of contraction, slower rates of epithelialization, and formation of exuberant granulation tissue (Hendrickson and Virgin, 2005; Theoret and Wilmink, 2013). The chronic healing pattern seen in equine limb wounds is a complex and multifactorial process, as several factors seem to contribute. These factors include hypoxia (Sørensen, 2014), persistent chronic inflammation (Bundgaard et al., 2016; Wilmink et al., 1999), presence of biofilm (Jorgensen et al., 2017) and, differential gene/protein expression (Miragliotta et al., 2008a; Miragliotta et al., 2008b). *In vitro* studies showed that fibroblasts from equine limb skin have dissimilar responses to different growth factors than fibroblast from the oral mucosa, which might be contributing to the different healing responses at these locations (Rose, 2012; Watts and Rose, 2012). It is possible that also other anatomical/phenotypical differences might contribute to the differences observed during wound repair.

To improve our understanding of equine skin conditions and wound healing it is thus important to obtain more information on the microanatomy and to understand how normal keratinocytes

differentiate and proliferate in equine skin at different locations. The objective of this study was to characterize the normal morphology of body and limb skin of horses. Morphology was studied by morphometrical and immunohistochemical approaches: epidermal thickness and keratinocyte proliferation rate were measured, the expression of cytokeratin (CK) 10, CK14, CK16, loricrin, and peroxisome proliferator-activated receptor-α (PPAR-α) and loricrin were evaluated, and a morphometric analysis of mast cell distribution was performed.

2. Materials and methods

2.1. Animals and samples

Eight mm skin punch biopsies were collected from six adult horses. The horses were clinically healthy and were without any signs or history of dermatological diseases or injuries. The horses were sedated and received local analgesia before the biopsies were obtained. Samples were obtained from the lateral metacarpus, lateral metatarsus, and from the thorax just caudal to the triceps muscle. The samples were placed in 4% formaldehyde for fixation before embedding in paraffin wax. The experimental protocol was approved by the Danish Animal Experiments Inspectorate (license no. 2016-15-0201-00981), and procedures were carried out per the Danish Animal Testing Act and the EU Directive 2010/63/EU for animal experiments.

2.2. General morphology and epidermal thickness

For histological evaluation and epidermal thickness measurements body, front, and hind limb skin sample sections stained with haematoxylin and eosin were used. The sections were first assessed by light microscopy for qualitative assessment of morphological features (epidermis, pigment, hair follicles, sebaceous glands, sweat glands, and dermis). Epidermal thickness was measured as previously reported by Abramo and colleagues (2016). Briefly, on ten 400× captured fields, 16 segments, at regular intervals per captured field, were traced with NIS-Elements Br Microscope Imaging Software (NIS-Elements Br Microscope Imaging Software, Nikon Instruments, Calenzano, Italy). Segments were perpendicular to the basement membrane and extended from the basement membrane to the beginning of the stratum corneum.

92 **2.3. Immunohistochemical analyses of skin samples**

93 Sections (4 µm) were cut and deparaffinized using a standardized method by immersing the glass
94 slides in xylene (3x5 min), 99% ethanol (2x5 min), 95% ethanol (2x5 min), 70% ethanol (1x5 min),
95 and in distilled water (2x5 min). To investigate the spatial distribution of CK10, CK14, CK16,
96 loricrin, and PPAR-α indirect immunofluorescence was performed. For Ki-67 (cell proliferation
97 marker) and mast cell tryptase, sections were stained by the immunoperoxidase method. All
98 commercial antibodies used are displayed in table 1.
99 Primary antibodies were applied after heat-induced epitope retrieval, 1% hydrogen peroxide
100 treatment (only for immunoperoxidase method), and standard blocking. Antibodies were left for 19
101 hours at 4 °C. After washing in PBS (4x10 min) secondary antibodies were applied for one hour.
102 After washing in PBS (3x10 min) sections for fluorescence were mounted with a mounting media
103 containing DAPI (Vectashield® Hard Set mounting media with DAPI, Vector Laboratories,
104 Burlingame, California) and sections for peroxidase had ABC reagent (Vectastain® R.T.U Elite®
105 ABC reagent, Vector Laboratories, Burlingame, California) applied for 45 min at room temperature.
106 After another wash in PBS (3x10 min) the peroxidase sections were developed using DAB reagent
107 (ImmPACT^{TM} DAB peroxidase substrate kit, Vector Laboratories, Burlingame, California) for 120
108 sec. After that, sections were dehydrated in increasing alcohol gradients, cleared in xylene and
109 mounted with permanent mounting medium (DPX mountant for microscopy, BDH – VWR
110 International Ltd., Poole, England). Immunohistochemistry was performed on hind limb and body
111 samples, but not on front limb samples, as no differences in general morphology and epidermal
112 thickness were discovered between front and hind limb skin.
113 The epidermal proliferation index (Ki-67 immunostaining) was calculated after counting the
114 number of positively stained basal keratinocytes related to number of total basal keratinocytes

throughout the skin biopsy. Values were expressed as percent of positive cells out of the total basal cells.

Microscopic examinations of immunofluorescence tissue sections were performed by using a fluorescence microscopy (Nikon Eclipse 80i, Nikon Instruments, Calenzano, Italy) and the accompanying software (NIS-Elements Br Microscope Imaging Software, Nikon Instruments, Calenzano, Italy).

2.4. Mast cell morphometry

As described in section 2.3 immunohistochemistry was performed on body and limb skin samples with the primary antibody against mast cell tryptase. Visualization and morphometric analysis were performed under a standard light microscope (Nikon Ni-e, Nikon Instruments, Calenzano, Italy) at x100 magnification using the accompanying software (NIS-Elements Br Microscope Imaging Software, Nikon Instruments, Calenzano, Italy). The positive cells were counted in two different areas throughout the dermis in accordance with a previously reported method (van der Haegen et al., 2001): the subepidermal layer (here defined as 0-325 µm below the basal membrane) and the deep dermis (325-975 µm below the basal membrane), and were expressed as number of cells / mm^2.

2.5. Statistical analysis

All data handling was done using Microsoft Excel 2010, and paired t-tests and one way ANOVA analyses were performed using GraphPad Prism version 5.01 (GraphPad Software, San Diego California, USA). Data are reported as means ± SD. For non-normally distributed data (mast cell tryptase positive cells) data are presented as median (range) and analyzed using Wilcoxon signed

rank test in SAS Enterprise Guide 7.13 (SAS Institute Inc., Cary, NC, USA). A significance level of $P < 0.05$ was chosen for this study.

3. Results

3.1. General morphology, epidermal thickness and keratinocyte proliferation

Body and limb skin samples showed an epidermis composed of stratified keratinocytes with melanin confined to the basal layer. Two-four and four-six layers of keratinocytes were present in body and limb skin, respectively. Hair follicles were primarily in the anagen phase. Arrector pili muscles, sebaceous glands, and sweat glands were present in all samples. Sebaceous glands showed a multivacuolated cytoplasm with nuclei centrally located. Dermis showed the presence of thinner collagen bundles in the subepidermal area (papillary dermis) compared to thicker bundles seen in the underlying parts (reticular dermis). Below the reticular dermis a cordovan layer was observed in both areas while, in limb samples only, collagen bundles became thicker and formed an accessory layer (namely the third/accessory layer). Collagen bundle orientation in the accessory layer was parallel to the epidermal surface. These histological findings are displayed in Fig. 1. No pathological changes were observed in any of the samples.

The average epidermal thickness of the body skin was 29.36 μm ± 3.58 μm, for hind limb skin 46.22 μm ± 7.84 μm, and for front limb skin 46.76 μm ± 6.31 μm. There was a statistically significant difference between body skin and limb skin ($p < 0.01$), but no significant difference between hind limb and front limb epidermal thickness ($p = 0.10$).

The epidermal proliferation indices for body and limb skin were 7.42 ± 2.33 and 6.78 ± 3.16, respectively, which did not differ statistically significantly ($p = 0.69$).

3.2. Epidermal differentiation markers

CK10 was found in keratinocyte suprabasal layers only. CK14 was found in basal layer keratinocytes as well as in suprabasal layers, where the staining fainted. CK16 was found in all

epithelial structures (epidermis, sweat and sebaceous glands, epithelial structures of hair follicles); in the epidermis, staining was most prominent in the basal and suprabasal keratinocytes. PPAR-α was found in the basal layer of the epidermis, in endothelial cells, and in perivascular subepidermal cells. CK10, CK14, CK16 and PPAR-α were always observed as cytoplasmic staining. These findings were similar for body and limb skin. Loricrin also showed a cytoplasmic localization and was present in the granular layer only in body skin, but in limb skin multifocal areas with loricrin extending into the suprabasal layers were found in 4 out of 6 horses (67 %). Immunohistochemical findings are displayed in Fig. 2.

3.3. Mast cell morphometry

In the subepidermal layer 54.3 (18.2-101.1) mast cells/mm^2 were found in body samples and 38.1 (2.4-103.7) mast cells/mm^2 were found in limb samples, there was no statistical difference between the different areas ($p = 0.59$). In the deeper dermis 21.7 (8.6-38.4) mast cells/mm^2 were found in body samples and 23.9 (15.0-32.5) mast cells/mm^2 were found in limb samples, there was no statistical difference between the different areas ($p = 0.81$). Taken together, there were significantly more mast cell tryptase positive cells per mm^2 in the subepidermal layer than in the deeper dermal layer ($p = 0.04$). Representative images of tryptase immunohistochemistry are shown in Fig. 3.

4. Discussion

Skin samples included in the study showed normal skin morphology similar to that reported previously (Talukdar et al., 1972a). Equine dermal microscopic structure has been studied by other investigators: the different appearance of collagen fibers described in the present study can be referred to the papillary (superficial) dermis, reticular dermis, cordovan layer and third/accessory cordovan layer (Wakuri et al., 1995). The latter was found exclusively in limb samples in our study. It is not clear how localization of the accessory cordovan layer in equine skin could affect pathological responses in the skin.

In 1972 Talukdar and colleagues investigated epidermal thickness of different body areas from 13 horses using an ocular micrometer, but unfortunately, the study did not assess metacarpal or metatarsal epidermal thickness. The thickness of the body epidermis (in the costal region) was 46 µm, i.e. considerably thicker that the 29.36 µm recorded for thoracic skin in our study. These differences can be due to different equipment and techniques used for the measurements. The consequences of the thicker epidermis observed in the equine limb compared to that of body skin needs to be evaluated, but it may affect stiffness/elasticity of the skin and thereby retraction and contraction of skin in wound healing since, as reported earlier (Wakuri et al., 1995), it comprises elastic fibers interwoven to collagen fibers.

Cytokeratins are important structural proteins of the cytoskeleton of epithelial cells, including keratinocytes. The keratinocyte differentiation markers CK10 and CK14 were expressed as expected (in the suprabasal and basal layers, respectively) based on previous reports on normal equine epithelium (Pastar et al., 2014). In skin from horses suffering from chronic pastern dermatitis with moderate to marked epidermal hyperplasia, abnormal keratinocyte differentiation was evident with decreased expression of CK10 and CK14 in the suprabasal and basal layers, respectively, and increased expression of CK14 in the suprabasal layers (Geburek et al., 2005).

These findings indicate that expression patterns of cytokeratin are changed during skin disease in horses. Surprisingly, CK16 was present in normal epithelia, which is contrary to human skin, where CK16 is only found in activated keratinocytes in the epidermis as part of the wound healing process or during hyperproliferation (Freedberg et al., 2001; Jiang et al., 1993). Species-differenced in CK expression has been demonstrated previously, as Walter (2001) demonstrated CK6, expressed only in activated cells in human skin, to be present in basal and suprabasal layers of normal canine skin. These species differences could reflect the tension placed on skin, the presence of CK16 in skin has been suggested to be a stabilization mechanism against increased load (Jiang et al., 1993; Walter, 2001), which may be higher in horses than in humans.

As loricrin is a terminal differentiation marker, it was detected as expected in the granular layer of the epidermis (Liang et al., 2012). However multifocal dystrophic deposits in deeper layers were observed in four out of six limb skin samples. Loricrin has a defensive and protective function in the epidermis (Nithya et al., 2015). The expression of loricrin is increased in a group of disorders (palmo plantar keratoderma) in humans, where hyperkeratosis occurs on soles and palms; in patients suffering from these disorders loricrin is expressed in more cell layers than normal (Nithya et al., 2015). Multifocal dystrophic loricrin deposits in deeper layers of in the equine limb epidermis could be a sign of increased stress and loading of the skin in this area, but could also be an artifact caused by oblique sectioning of hair follicles in limb skin, as these contain loricrin in their walls. Future studies should investigate this by staining skin section cut strictly parallel to the epidermal surface.

PPAR-α is a nuclear receptor that regulates metabolism. As reported for human skin (Westergaard et al., 2003), PPAR-α was found in the cytoplasm of the basal keratinocytes in equine skin. While its functions have never been investigated in horses, PPAR-α is down regulated in atopic dermatitis

and some skin cancers in humans (Sertznig et al., 2008); and in a murine wound model PPAR was described to play a role in re-epithelialization (Michalik et al., 2001).

The epidermal proliferation index has not been reported in horses before, but expression of Ki-67 has been used to document proliferation in an equine *in vitro* skin model (Cerrato et al., 2014) and in stem cell treatment of equine wounds (Broeckx et al., 2014). In human and veterinary medicine, the epidermal proliferation (Ki-67) index has been used to diagnose and prognosticate skin tumors (Marinescu et al., 2016), including canine and equine mast cell tumors (Halse et al., 2014; Maglennon et al., 2008). The normal epidermal proliferation (Ki-67) index of equine skin reported here can be used as normal value in diagnostic equine dermatology.

The amount of mast cell tryptase positive cells per mm^2 in the different compartments of the skin in this study was very much in line with findings of van der Haegen and colleagues (2001), where biopsies from mane/tale base were analyzed. Also in canine skin, more mast cells are present in the subepidermal dermis compared to deeper dermis (Auxilia and Hill, 2000). The presence of tryptase positive mast cells in the subepidermal dermis has in a human study (Huttunen et al., 2000) been associated with delayed wound healing and epithelialization. Involvement in equine healing should be further investigated, but as equine body and limb skin contained similar numbers of tryptase positive mast cells, it does not seem likely that they contribute to the delayed wound healing of equine limb wounds.

In conclusion, our study may serve as a basis to further studies aimed to investigate changes occurring in epidermal thickness, keratinocyte proliferation/differentiation and mast cell count during wound healing and other dermatopathological conditions affecting horses.

Authors' declaration of interest

No conflicts of interests.

Sources of funding

E.J. was funded by a Danish Government PhD grant, and the work was supported by the Augustinus foundation. The funding sources had no involvement on the research or the preparation of the manuscript.

Acknowledgements

Anti-CK16 was generously sponsored by Cloud-Clone Corp. (provided by DBA Italia srl).

260 **Table 1. Primary and secondary antibodies used for immunohistochemical analyses**

Primary antibodies					
Name	**Company**	**Number**	**Clonality**	**Host**	**Dilution**
Anti-CK16	Cloud-Clone Corp.	PAA516Hu01	Polyclonal	Rabbit	1:200
Anti-CK14	Abcam	Ab7800	Monoclonal	Mouse	1:200
Anti-CK10	Abcam	Ab9026	Monoclonal	Mouse	1:200
Anti-Loricrin	Abcam	Ab24722	Polyclonal	Rabbit	1:400
Anti-Ki-67	Dako	M7240	Monoclonal	Mouse	1:300
Anti-PPAR-α	Novusbio	NBP1-03288	Polyclonal	Rabbit	1:200
(Anti-Mast Cell Tryptase (AA1))	Santa Cruz Biotechnology	sc-59587	Monoclonal	Mouse	1:400
Secondary antibodies					
Name	**Company**	**Number**	**Host**	**Dilution**	
DyLight649 Anti-mouse IgG	Vector Laboratories	DI-2649	Horse	1:200	
DyLight488 Anti-mouse IgG	Vector Laboratories	DI-2488	Horse	1:200	
DyLight488 Anti-rabbit IgG	Vector Laboratories	DI-1088	Horse	1:200	
R.T.U. biotinylated universal antibody anti-rabbit/mouse	Vector Laboratories	BP-1400	Horse	RTU	

261

Legends for figures

Fig. 1: Photomicrographs of hematoxylin and eosin stained sections of equine body (a) and limb (b) skin: p = papillary dermis, r = reticular dermis, arrowheads indicate sebaceous glands and asterisk indicate apocrine sweat glands. (c) High magnification of a hair bulb in the anagen phase of cycling, asterisk indicate apocrine sweat gland. (d) High magnification of a sebaceous gland showing a multivacuolated cytoplasm with centrally located nucleus. (e-f) Low and high magnification respectively of the deep dermis of limb skin showing the cordovan layer (cl) and the third/accessory layer (t). Scale bars are equal to 400 µm (a, b, e), 100 µm (c-d), or 50 µm (f).

Fig. 2: Photomicrographs of equine skin samples stained with cytokeratin (CK)10, CK14, CK16, loricrin and PPAR-α. Different colors are explained within the figure. (a-g) Epidermal immunostaining. (h) CK16 is present in all the epithelial structures in the dermis (hair follicles, sebaceous, and sweat glands). Left images are from body skin samples while right images are from limb skin. Scale bars are equal to 50 µm (a-f) or 200 µm (h).

Fig. 3: Photomicrographs showing tryptase immunostaining for mast cells. (a) Subepidemal mast cells indicated by arrowheads. (b) Arrowheads indicate mast cells intercalated to apocrine sweat glands (asterisk). (c-d) Low and high magnification respectively of a hair bulb focusing on the hair papilla were several mast cells are visible (indicated by arrowheads). Inset in (c) shows toluidine blue stained mast cells within hair papilla. (e-f) Third/accessory cordovan layer vascular plexuses (asterisks) with perivascular mast cells (arrowheads). Scale bars are equal to 50 µm (a, b, d, f) or 100 µm (c, e).

References

Anonymous. Equine 2015, Section 1C: Baseline Reference of Equine Health and Management in the United States 2015. https://www.aphis.usda.gov/animal_health/nahms/equine/downloads/equine15/Eq2015_Rept1.pdf (accessed 10th of October 2017). United States Department of Agriculture, Fort Collins, CO, USA, 2016.

Abramo, F., Pirone, A., Lenzi, C., Vannozzi, I., Della Valle, M.F., Miragliotta, V., 2016. Establishment of a 2-week canine skin organ culture model and its pharmacological modulation by epidermal growth factor and dexamethasone. Ann. Anat. 207, 109-17.

Auxilia, S.T., Hill, P.B., 2000. Mast cell distribution, epidermal thickness and hair follicle density in normal canine skin: possible explanations for the predilection sites of atopic dermatitis? Vet. Dermatol. 11, 247-254.

Broeckx, S.Y., Maes, S., Martinello, T., Aerts, D., Chiers, K., Marien, T., Patruno, M., Franco-Obregon, A., Spaas, J.H., 2014. Equine Epidermis: A Source of Epithelial-Like Stem/Progenitor Cells with In Vitro and In Vivo Regenerative Capacities. Stem Cells Dev. 23, 1134-1148.

Bundgaard, L., Bendixen, E., Sorensen, M.A., Harman, V.M., Beynon, R.J., Petersen, L.J., Jacobsen, S., 2016. A selected reaction monitoring-based analysis of acute phase proteins in interstitial fluids from experimental equine wounds healing by secondary intention. Wound Repair Regen. 24, 525-532.

Cerrato, S., Ramio-Lluch, L., Brazis, P., Rabanal, R.M., Fondevila, D., Puigdemont, A., 2014. Development and characterization of an equine skin-equivalent model. Vet. Dermatol. 25, 475-477.

Freedberg, I.M., Tomic-Canic, M., Komine, M., Blumenberg, M., 2001. Keratins and the keratinocyte activation cycle. J. Invest. Dermatol. 116, 633-640.

Geburek, F., Ohnesorge, B., Deegen, E., Doeleke, R., Hewicker-Trautwein, M., 2005. Alterations of epidermal proliferation and cytokeratin expression in skin biopsies from heavy draught horses with chronic pastern dermatitis. Vet. Dermatol. 16, 373-384.

Halse, S., Pizzirani, S., Parry, N.M., Burgess, K.E., 2014. Mast cell tumor invading the cornea in a horse. Vet. Ophthalmol. 17, 221-227.

Hendrickson, D., Virgin, J., 2005. Factors that affect equine wound repair. Vet. Clin. North Am. Equine Pract. 21, 33-44.

313 Huttunen, M., Aalto, M.L., Harvima, R.J., Horsmanheimo, M., Harvima, I.T., 2000. Alterations in
314 mast cells showing tryptase and chymase activity in epithelializating and chronic wounds. Exp.
315 Dermatol. 9, 258-265.
316 Jatana, S., DeLouise, L.A., 2014. Understanding engineered nanomaterial skin interactions and the
317 modulatory effects of ultraviolet radiation skin exposure. Wiley Interdiscip. Rev. Nanomed.
318 Nanobiotechnol. 6, 61-79.
319 Jiang, C.K., Magnaldo, T., Ohtsuki, M., Freedberg, I.M., Bernerd, F., Blumenberg, M., 1993.
320 Epidermal growth factor and transforming growth factor alpha specifically induce the activation-
321 and hyperproliferation-associated keratins 6 and 16. Proc. Natl. Acad. Sci. USA 90, 6786-6790.
322 Jorgensen, E., Bay, L., Bjarnsholt, T., Bundgaard, L., Sorensen, M.A., Jacobsen, S., 2017. The
323 occurrence of biofilm in an equine experimental wound model of healing by secondary intention.
324 Vet. Microbiol. 204, 90-95.
325 Liang, X., Bhattacharya, S., Bajaj, G., Guha, G., Wang, Z., Jang, H.S., Leid, M., Indra, A.K.,
326 Ganguli-Indra, G., 2012. Delayed cutaneous wound healing and aberrant expression of hair follicle
327 stem cell markers in mice selectively lacking Ctip2 in epidermis. PloS One 7, e29999.
328 Maglennon, G.A., Murphy, S., Adams, V., Miller, J., Smith, K., Blunden, A., Scase, T.J., 2008.
329 Association of Ki67 index with prognosis for intermediate-grade canine cutaneous mast cell
330 tumours. Vet. Comp. Oncol. 6, 268-274.
331 Marinescu, A., Stepan, A.E., Margaritescu, C., Marinescu, A.M., Zavoi, R.E., Simionescu, C.E.,
332 Niculescu, M., 2016. P53, p16 and Ki67 immunoexpression in cutaneous squamous cell carcinoma
333 and its precursor lesions. Rom. J. Morphol. Embryol. 57, 691-696.
334 Michalik, L., Desvergne, B., Tan, N.S., Basu-Modak, S., Escher, P., Rieusset, J., Peters, J.M., Kaya,
335 G., Gonzalez, F.J., Zakany, J., Metzger, D., Chambon, P., Duboule, D., Wahli, W., 2001. Impaired
336 skin wound healing in peroxisome proliferator-activated receptor (PPAR)alpha and PPARbeta
337 mutant mice. J. Cell Biol. 154, 799-814.
338 Miragliotta, V., Ipina, Z., Lefebvre-Lavoie, J., Lussier, J.G., Theoret, C.L., 2008a. Equine CTNNB1
339 and PECAM1 nucleotide structure and expression analyses in an experimental model of normal and
340 pathological wound repair. BMC Physiol. 8, 1.
341 Miragliotta, V., Lefebvre-Lavoie, J., Lussier, J.G., Theoret, C.L., 2008b. Equine ANXA2 and
342 MMP1 expression analyses in an experimental model of normal and pathological wound repair. J.
343 Dermatol. Sci. 51, 103-112.

344 Nithya, S., Radhika, T., Jeddy, N., 2015. Loricrin - an overview. J. Oral Maxillofac. Pathol. 19, 64-
345 68.
346 Owen, K.R., Singer, E.R., Clegg, P.D., Ireland, J.L., Pinchbeck, G.L., 2012. Identification of risk
347 factors for traumatic injury in the general horse population of north-west England, Midlands and
348 north Wales. Equine Vet. J. 44, 143-148.
349 Pastar, I., Stojadinovic, O., Yin, N.C., Ramirez, H., Nusbaum, A.G., Sawaya, A., Patel, S.B.,
350 Khalid, L., Isseroff, R.R., Tomic-Canic, M., 2014. Epithelialization in Wound Healing: A
351 Comprehensive Review. Adv. Wound Care 3, 445-464.
352 Rose, M.T., 2012. Effect of growth factors on the migration of equine oral and limb fibroblasts
353 using an in vitro scratch assay. Vet. J. 193, 539-544.
354 Sertznig, P., Seifert, M., Tilgen, W., Reichrath, J., 2008. Peroxisome proliferator-activated receptors
355 (PPARs) and the human skin: importance of PPARs in skin physiology and dermatologic diseases.
356 Am. J. Clin. Dermatol. 9, 15-31.
357 Sørensen, M.A., 2014. Hypoxia as a cause of exuberant granulation tissue formation in equine limb
358 spunds healing by second intention, Faculty of Health and Medical Science. University of
359 Copenhagen.
360 Sørensen, M.A., Pedersen, L.J., Bundgaard, L., Toft, N., Jacobsen, S., 2014. Regional disturbances
361 in metabolism and blood flow in equine limb wounds healing with formation of exuberant
362 granulation tissue. Wound Repair Regen. 22, 647-653.
363 Talukdar, A.H., Calhoun, M.L., Stinson, A.W., 1972a. Microscopic anatomy of the skin of the
364 horse. Am. J. Vet. Res. 33, 2365-2390.
365 Talukdar, A.H., Calhoun, M.L., Stinson, A.W., 1972b. Specialized vascular structure in the skin of
366 the horse. Am. J. Vet. Res. 33, 335-338.
367 Theoret, C.L., Barber, S.M., Moyana, T.N., Gordon, J.R., 2001. Expression of Transforming
368 Growth Factor β1, β3, and Basic Fibroblast Growth Factor in Full-Thickness Skin Wounds of
369 Equine Limbs and Thorax. Vet. Surg. 30, 269-277.
370 Theoret, C.L., Bolwell, C.F., Riley, C.B., 2016. A cross-sectional survey on wounds in horses in
371 New Zealand. N. Z. Vet. J. 64, 90-94.
372 Theoret, C.L., Wilmink, J.M., 2013. Aberrant wound healing in the horse: Naturally occurring
373 conditions reminiscent of those observed in man. Wound Repair Regen. 21, 365-371.

van der Haegen, A., Griot-Wenk, M., Welle, M., Busato, A., von Tscharner, C., Zurbriggen, A., Marti, E., 2001. Immunoglobulin-E-bearing cells in skin biopsies of horses with insect bite hypersensitivity. Equine Vet. J. 33, 699-706.

Wakuri, H., Mutoh, K., Ichikawa, H., Liu, B., 1995. Microscopic anatomy of the equine skin with special reference to the dermis. Okajimas Folia Anat. Jpn. 72, 177-183.

Walter, J.H., 2001. Cytokeratins in the canine epidermis. Vet. Dermatol. 12, 81-87.

Watts, E.J., Rose, M.T., 2012. Extracellular matrix expression by equine oral and limb fibroblasts in in vitro culture. Res. Vet. Sci. 92, 213-218.

Westergaard, M., Henningsen, J., Johansen, C., Rasmussen, S., Svendsen, M.L., Jensen, U.B., Schroder, H.D., Staels, B., Iversen, L., Bolund, L., Kragballe, K., Kristiansen, K., 2003. Expression and localization of peroxisome proliferator-activated receptors and nuclear factor kappaB in normal and lesional psoriatic skin. J. Invest. Dermatol. 121, 1104-1117.

Wilmink, J.M., Van Weeren, P.R., Stolk, P.W.T., Van Mil, F.N., Barneveld, A., 1999. Differences in second-intention wound healing between horses and ponies: histological aspects. Equine Vet. J. 31, 61-67.

Wobeser, B.K., 2015. Skin Diseases in Horses. Vet. Clin. North Am. Equine Pract. 31, 359-376.

Figure 1

Click here to download high resolution image

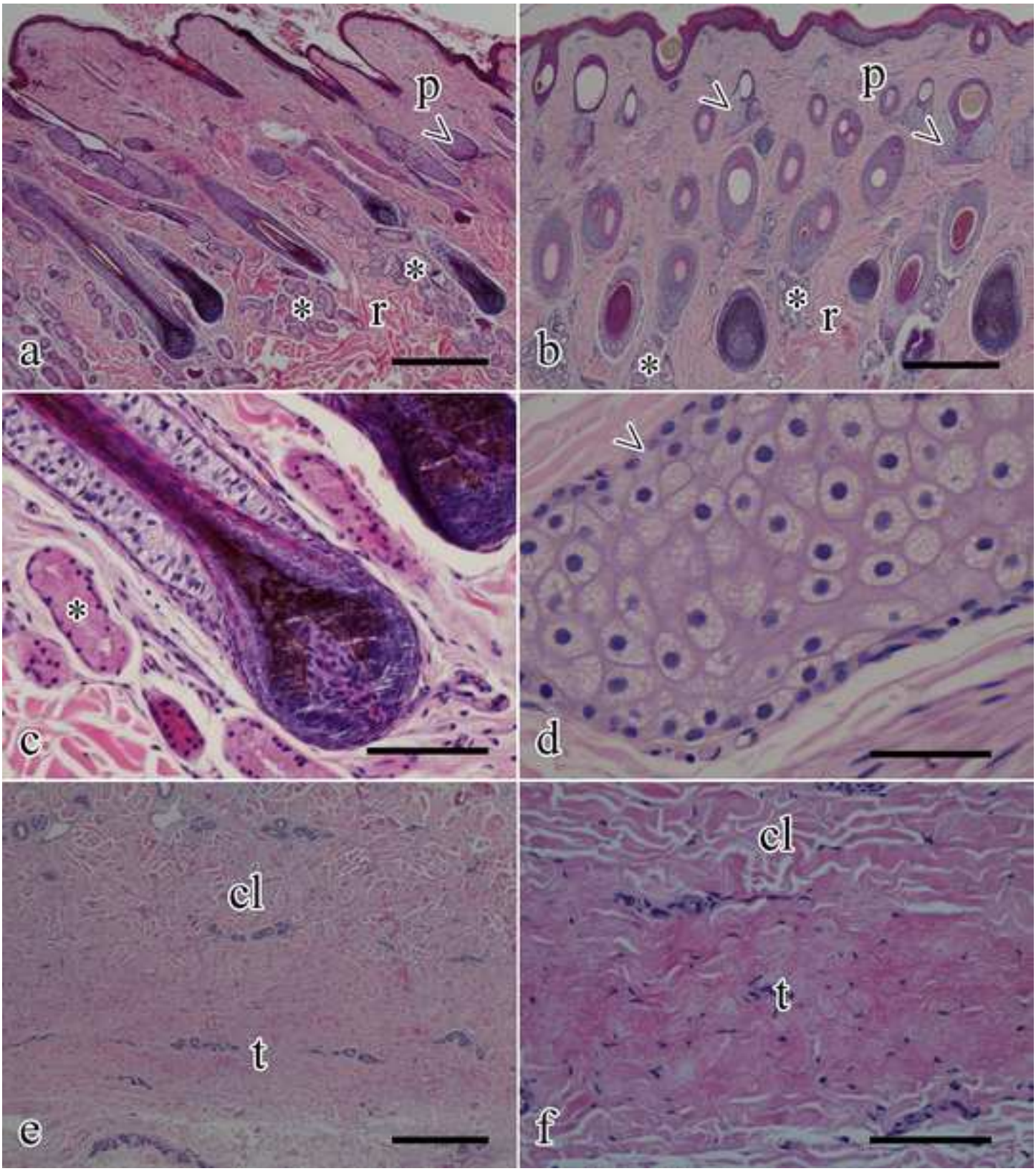

Figure 2

Click here to download high resolution image

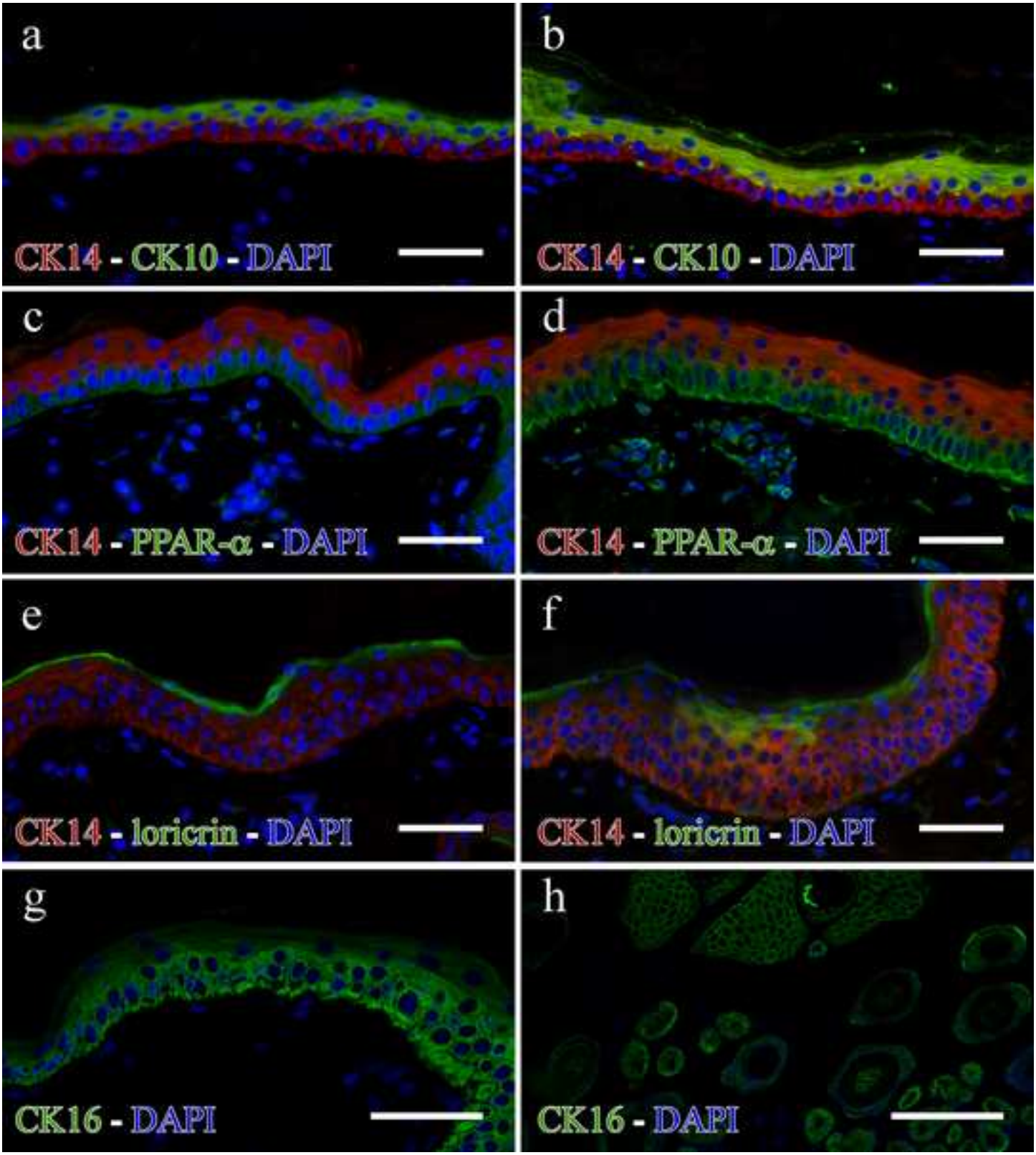

Figure 3

Click here to download high resolution image